

Wind Velocity Field during Thunderstorms, Extreme Wind Velocities in Mixed Wind climates and new data from intense downburst

Jorge D. Riera

PPGEC, EE, Universidade Federal do Rio Grande do Sul, Porto Alegre, RS, Brasil
Av. Osvaldo Aranha 99, 3o. Andar, 90035-970, Porto Alegre, RS, Brasil

[<jorge.riera@ufrgs.br>](mailto:jorge.riera@ufrgs.br)

1. INTRODUCTION

Wind action is usually a factor of fundamental importance in structural design, especially in case of large spans and light structures. Codes for structural design assume that in flat terrain the incident mean wind velocity vector is parallel to the ground, which constitutes a valid simplification for winds caused by the most frequent meteorological phenomena, such as Extratropical Storms, herein designated Extended Pressure Systems (*EPS*) or Tropical Storms (Hurricanes, Typhoons). On the other hand, wind effects due to other phenomena, such as downbursts during thunderstorms (*TS*), and its combination with *EPS* winds in so-called squall lines, are simply neglected. In these events, the spatial distribution of the wind velocity maximum amplitude on any horizontal plane, as well as its orientation, are far from uniform. Thus, *TS* wind fields differ significantly from models implicit in current codes, rendering the applicability of the latter to large constructions highly questionable. Moreover, *TS* wind records can no longer be regarded as samples of a *stationary* random process and it seems unlikely that the along-wind fluctuating velocity components are governed by surface roughness, as in case of *EPS* winds. Since the vertical velocity profiles are also different, both static and dynamic methods of analysis of tall, flexible structures subjected to wind action presently in use are not adequate to model the excitation due to *TS* events.

In temperate latitudes, in regions *not affected by tropical cyclons*, while roughly nine out of ten maximum annual velocity records at the standard 10m observation height occur during *EPS* events, extreme winds for design periods longer than about ten years are typically caused by *TS* events. In fact, Riera *et al* [22] underlined a quarter of a century ago the need to assess the probability distribution of extreme *thunderstorm* wind velocities, sustained by the premise that the probability distribution of the maximum annual *TS* wind velocity at the reference 10m height must be different from the distribution functions that describe the probability of occurrence of winds caused by extratropical or by tropical storms. Thom [28] had earlier proposed to deal with mixed populations of *EPS* and tropical storm winds by resorting to a combined probability distribution $P_V(v)$. At any rate, Riera and Nanni [23] confirmed, using data from 14 meteorological stations in southern Brazil that extreme annual *EPS* and *TS* winds are characterized by different probability distributions and that *TS* govern the low probability region.

The frequency and magnitude of damage caused by thunderstorms, on the other hand, called the attention of engineers engaged in transmission line design and maintenance. In fact, more that 80% of transmission line tower failures due to wind action in temperate climates occur during thunderstorms [6]. This evidence confirms the importance of *TS* winds in structural design, and justifies the growing interest in the phenomenon, which actually begun in aeronautical engineering. In this paper, a simplified model of the 3D wind field caused by a downdraft during a *TS* event is proposed, which accounts for the transient nature

of *TS* winds as well as for its *fluctuating* components. An application of the model to simulate the wind climate associated to *TS* winds is described next. Simulations of this type may be useful in the design or risk analysis of transmission lines, long-span crossings, cable-stayed bridges and similar structures. Finally, the overview of developments and current research at LDEC is completed with records obtained during a *TS* event in Passo Fundo.

2. RECENT DEVELOPMENTS AT LDEC IN RELATION TO *TS* WINDS

In a previous paper, the author described a non-stationary model of the wind field in a *TS* event, Ponte [20], Ponte and Riera [21], which is formulated in terms of meteorological variables, such as the height over the ground surface of the bottom of the causative cumulonimbus cloud and the diameter of the downdraft cylinder or the pressure drop, for which scarce data is available and no probabilistic model known to the authors exists. Nevertheless, the potential applications of these models, both for design purposes of special engineering constructions, such as power lines, elevated railway systems or long span bridges, as well as in the context of reliability assessments, are quite large.

The applications mentioned above include, for example, the generation by Monte Carlo simulation of all the meaningful events causing high winds along an entire transmission line during its lifetime. Note that in each loading case no additional simplifying assumptions concerning wind orientation, spatial distribution of the velocity or storm duration would be necessary. In connection with extreme velocity predictions at sites of interest and structural reliability assessments, an interesting use of the model is the simulation of extreme annual wind velocities, in terms of meteorological variables that are generally available, as the number of *EPS* or *TS* events per year at the location of interest. This would allow the estimation of the probability distribution of the wind velocity at sites that are distant from meteorological stations or where only short duration records are available.

By way of illustration, the simulation of extreme annual wind velocities caused by *TS* events at the standard 10m reference height at two sites in southern Brazil is described next. The probability density functions obtained by simulating 50 years of record are compared with predictions based on actual observations at meteorological stations located at the selected sites [23], [24]. It is shown that the differences between both approaches are compatible with the expected statistical errors and that the proposed model may be used with confidence in engineering applications. It is nevertheless unquestionable that the proposed model can be improved by new data on the relevant random variables as well as in the description of the wind field itself. These improvements or eventual corrections would require the contribution of specialists in other areas, such as boundary layer meteorology, computational meteorology and fluid dynamics, and it is hoped that this paper will promote cooperation.

3. PROBABILITY DISTRIBUTION OF EXTREME ANNUAL *TS* WIND VELOCITY

Nearly three decades ago, Riera *et al* [22] advanced a proposal to assess the probability distribution of extreme *thunderstorm* (*TS*) wind velocities, expecting that the probability distribution of the maximum annual *TS* wind velocity at the reference 10m height should be different from the distribution functions that describe the probability of occurrence of winds caused by extratropical storms, herein designated *extended pressure systems* (*EPS*) or by tropical storms. In fact, Thom [27] had earlier proposed to deal with mixed populations of *EPS* and tropical storm winds by resorting to the combined probability distribution $P_V(v)$:

$$P_V(v) = P_E \exp[-(v/\beta)^9] + P_T \exp[-(v/\beta)^{4.5}] \quad (1)$$

in which P_T denotes the frequency of occurrence of tropical cyclons in the 5° longitude-latitude square under consideration and $P_E = 1 - P_T$. Thom [27] assumed the universal

validity of eq.(1), which requires, in a general case, the estimation of P_T and β . Gomes and Vickery [11], in turn, had suggested that the distribution of maximum annual wind velocities caused by *TS* events should be related to the mean number of storms per year n_s , proposing on the basis of observations at an Australian meteorological station the adoption of a Fisher-Tippett Type I distribution (Gumbel). Riera *et al* [22] proposed to assess annual extreme *TS* wind velocities by adopting a Fisher-Tippett II (Frechet) distribution with parameters:

$$\beta = 12.66 + 3.76 \ln n_s \quad (\text{m/s}) \quad (2)$$

$$\gamma = 3.36 + \ln n_s \quad (3)$$

It is recognized now that the *isolated* *TS* storm is less damaging than those occurring in a squall-line, in which a sum of effects takes place. Thus eqs. (2.-3) would have restricted applicability. Riera and Nanni [23] confirmed later that *EPS* and *TS* extreme annual wind series do present different probability distributions. When the registered velocities are classified according to their origin, in this case either *EPS* or *TS*, and angle of incidence, extreme type I distributions best fit the available series recorded at 8 Brazilian meteorological stations.

4. MODEL OF THE WIND FIELD DURING STATIONARY DOWNDRAFT

The model of the downdraft during a *TS* event described by Ponte and Riera [21] was adopted in this study. Readers interested in comparisons of the model predictions with other formulations or field observations may consult the reference cited above. It is assumed that, in case of a stationary cumulonimbus cloud, the wind field is axisymmetric and depends on the following physical parameters: pressure drop, background wind velocity, direction of background wind, height from level to the cloud anvil center, ratio of cloud base and characteristic time of the storm, which herein considered random variables.

A similar set of assumptions was adopted in wind tunnel studies of the phenomenon, in which a downburst was modelled by a stationary jet impinging on a flat surface (Wood & Kwok [12]). In this context, Riera and Rocha [8] proposed an axi-symmetric velocity field based on a solution developed by Zhu & Etkin [13]. Similar models are due to Holmes and Oliver [14] and Chen and Lechford [15]. The axi-symmetric velocity field [8] constitutes a satisfactory approximation to a stationary downdraft and was adopted with some simplifications in the *TS* transient wind field proposed by Ponte and Riera [5]. The latter is a basic tool in the simulation study discussed herein and will thus be summarized in the following. It is assumed that the causative cumulonimbus cloud is a circular cylinder with vertical axis. The base of the cylinder, *i.e.* of the cloud, is at height h above ground level. The flow lines are also assumed to be axisymmetrical in relation to the cloud vertical axis.

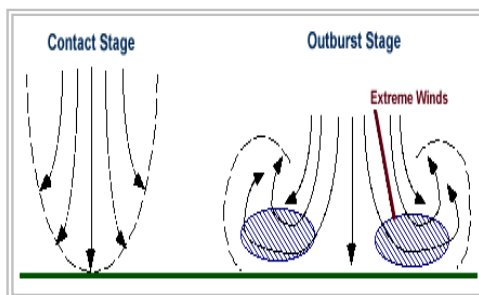


Figure 1. Flow lines in *TS* (initial contact)
(From University of Illinois - WW2010 on line guides)

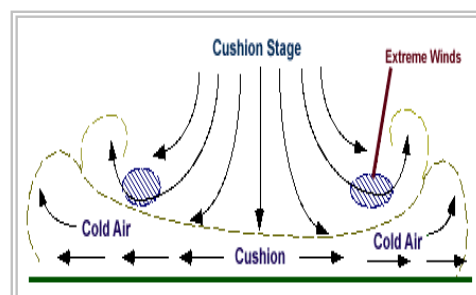


Figure 2. Flow lines in *TS*
(From University of Illinois - WW2010 on line guides)

Hence, applying Bernoulli's Theorem for heights h and z above the ground, the tangential velocity at height z along a flow line is obtained, in which dp denotes a pressure differential while ρ is the specific mass, modeled by the exponential function (5):

$$V_t = [2 \int (dp / \rho)]^{1/2} \quad (4)$$

$$\rho(z) = \rho_o \exp (-\beta z) \quad (5)$$

In the range $0 < z < 10000$ m the parameters in equation (3.2), estimated using data from Mc Donald & Fox [16], are $\rho_o = 1,019 \text{ kg/m}^3$ and $\beta = 0,0001$. The pressure difference is assumed to vary linearly from zero at height h to ΔP_o at ground level. The pressure at height z is:

$$p = \Delta P_o (1-z/h) \quad (6)$$

introducing equations (3.2) and (3.3) in equation (3.1) and solving the integral, the following expression for the tangential velocity is finally obtained:

$$V_t = [(2 \Delta P_o) / (h \rho_o \beta)]^{1/2} [\exp(\beta h) - \exp(\beta z)]^{1/2} \quad (7)$$

Furthermore, available information suggests that the total pressure drop ΔP_o ranges between 100 and 500 Pa. although no data was found to fit a probability density function to ΔP_o , which must then be modeled solely on the basis of its estimated maximum and minimum values. For any given value of ΔP_o , eq.(3.4) allows the determination of the tangential velocity. Typical velocity-height curves are shown in Fig. (3). The axial and radial velocity components along a flow line can be determined from equation of the latter. Zhu & Etkin [31] presented a simplified 3-dimensional model –the so called *doublet sheet model*- based on fluid mechanics considerations. For engineering purposes, the model was simplified, maintaining the assumption of axial symmetry. In the following the flow lines are described by eq. (8), in which k is a constant and r is the distance to the vertical axis of the cloud.:

$$z(r) = k/r \quad (8)$$

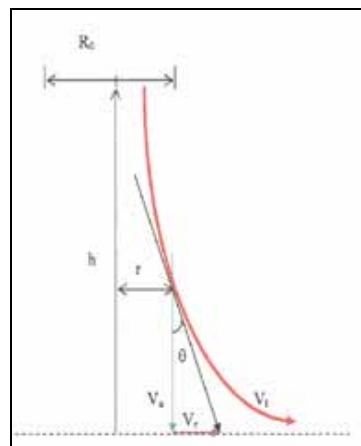


Figure 3 - Flow line in downdraft

In fact, for various similar flow lines, differences in predicted velocities are marginal. For a specific flow line, the derivative of z in relation to r , denoted $z'(r)$ defines the tangent of the angle in relation to the Or axis. At point (r_p, h) , the radial and axial velocity components for any height z of interest are given by:

$$V_r = V_t \{ 1/[1+z^2(r_p)] \}^{1/2} \quad (9)$$

$$V_a = V_t \{ z^2(r_p)/[1+z^2(r_p)] \}^{1/2} \quad (10)$$

$$r = [x^2 + y^2]^{1/2} \quad (11)$$

$$\sin \theta = \{ 1/[1+z^2(r_p)] \}^{1/2} \quad (12)$$

$$\cos \theta = \{ z^2(r_p)/[1+z^2(r_p)] \}^{1/2} \quad (13)$$

in which θ denotes the angle between the tangent to the flow line and the vertical axis Oz . Finally, it results:

$$V_a = V_t [r_p^2 h^2 / (r_p^2 h^2 + r^4)]^{1/2} \quad (14)$$

$$V_r = V_t [r^4 / (r_p^2 h^2 + r^4)]^{1/2} \quad (15)$$

The velocity components in the direction of the coordinate axes are given by:

$$V_x = V_t \sin \theta \cos \beta = V_r \cos \beta \quad (16)$$

$$V_y = V_t \sin \theta \sin \beta = V_r s \quad (17)$$

$$V_z = V_t \cos \theta = V_a \quad (18)$$

In which β denotes the angle between the projection of the flow line on a horizontal plane and the Ox axis.

5. BACKGROUND WIND AND TRANSLATIONAL VELOCITY OF CAUSATIVE CLOUD

In most cases, the causative cloud is carried by the general circulation in the region, herein designated *background wind*. It is assumed that the background wind has constant velocity and the same orientation throughout the region in which the wind climate will be simulated, in this study a 400 km² square area. In rarer occasions, however, mature cumulonimbus clouds are carried by storm fronts. This gives rise to so-called *squall lines*, which result in higher wind intensities because the velocity resulting from the downdraft adds up to the translation velocity of the storm. In temperate latitudes, like southern South America, these fronts are due to extended pressure systems (EPS), *i.e.* extratropical cyclons, characterized by diameters that vary between around 400 and 1000 km. In view of those dimensions, it may be assumed that the velocity within the reference area, only 20 km wide, is uniform, although characterized by a probability distribution and turbulence that differ from those assigned to the background wind caused by general circulation. It is also assumed that the resulting velocity vector at any point may be obtained as the vectorial sum of the stationary velocity vector, determined in Section 3, and the background or EPS wind velocity vector. If V_o denotes the modulus of the wind velocity vector at a point, which forms an angle γ with the Ox axis, then the resultant velocity components in a reference cartesian coordinate system (xyz) are given by:

$$V_{Rx} = V_r \cos \beta + V_o \cos \gamma \quad (19)$$

$$V_{Ry} = V_r \sin \beta + V_o \sin \gamma \quad (20)$$

$$V_{Rz} = V_z \quad (21)$$

4.1 Evolution of the wind velocity with time. The wind velocity field described above assumes that the downdraft flow from the causative cloud is stationary. The resulting velocity amplitudes are thus upper bounds of the actual amplitudes, which vary with time defining a transient process. Following Holmes and Oliver [12], the evolution of the wind velocity with time is herein represented by the equations:

$$V(t) = 1,58 V_t [1 - \exp(-t/T)] \quad , \text{ for } t \leq T \quad (22)$$

$$V(t) = V_t \exp[-(t-T)/T] \quad , \text{ for } t > T \quad (23)$$

T denotes the storm *characteristic time*, defined as the time lapsed from the initiation of the transient wind to the instant at which the velocity attains its maximum value (See Fig. 4).

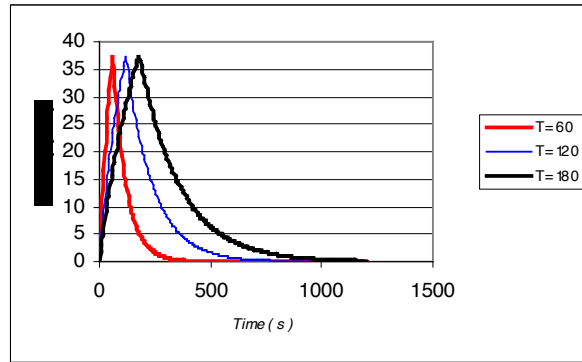


Figure 4. Velocity-time functions in terms of T

6. VERTICAL PROFILE OF HORIZONTAL VELOCITY COMPONENT

The *vertical profile of the horizontal component* of the wind velocity field at a given location has great interest in structural engineering, since it has a direct influence on the distribution of horizontal wind forces along the height of a construction at the location under consideration. The model proposed herein predicts a vertical profile, for a stationary cloud, similar to the graph of radial velocities shown in figure 6. It may be seen that the profile depends on the position of the vertical axis of the cloud in relation to the location of interest. Also note that the velocity distribution illustrated by Fig.6 does not take into account the roughness of the terrain, *i.e.* the existence of a boundary layer that would imply a decrease of the velocity as we approach the ground. Chen & Letchford [8] recently presented a critical evaluation of models of the vertical profile for *TS* winds available in the literature. Oseguera & Bowles [17] propose an empirical equation (24) for the average horizontal velocity caused by a downdraft:

$$V(z) = (\lambda R^2 / 2r) \{1 - \exp[-(r/R)^2]\} [\exp(-z/z_c) - \exp(-z/z_d)] \quad (24)$$

In which λ denotes a scale factor with dimension $[T]^{-1}$, z_d a characteristic height (inside the boundary layer), z_c a characteristic height (outside the boundary layer), r the distance to the vertical axis of the downdraft cylinder and R the characteristic radius of the downdraft cylinder. Vicroy [29], suggests the following equation for the velocity vertical profile:

$$V(z) = 1,22 V_{max} [\exp(-0,15 z / z_m) - \exp(-3,2175 z / z_m)] \quad (25)$$

In eq. (25), V_{max} is the maximum velocity in the profile, while z_m denotes the height at which the maximum velocity occurs. A third model is due to Wood & Kwok [30]:

$$V(z) = 1,55 V_{max} (z/z_0)^{1/6} \{ 1 - \Phi[0,7(z/z_0)] \} \quad (26)$$

In eq. (26), z_0 represents the height where the speed is half the maximum value while Φ denotes the error function. Chen e Lechtford [8] built comparative profiles of the models listed above. More recently Chay *et al* [7] proposed equation (27) for the vertical profile:

$$V(z) = (\lambda r / 2) [\exp(c_1(z/z_m)) - \exp(c_2(z/z_m))] \exp[(2 - (r^2 / r_p^2)^\alpha) / 2\alpha] \quad (27)$$

In which λ is a scale factor, α , c_1 and c_2 are constants, r is the radius r_p the radius at which the maximum velocity occurs, z_m the elevation at which the maximum velocity occurs and z a generic elevation. Figures 5 to 6 show vertical profiles proposed in the literature, which are compared with profiles predicted by the model described in this paper. The graphs were normalized to present in Fig. 6 a common velocity of 80 m/s at a 67 m height. It may be seen that although the various models reflect specific features of *EPS* winds, such as the fact that the maximum velocity is attained at a height usually below 100m and that the velocity decreases for higher elevations, they present perceptible differences. The present proposal approaches the model of Oseguera & Bowles [17] when the distance to the cloud axis is around 100m. When the distance is about 200m the model predictions approach Vicroy's [29] equation. The model predictions are not close to Wood & Kwok [30] results for any value of r . This poor correlation is attributed to the fact that the latter is based on experimental observations in wind tunnel, which do not faithfully reflect the field situation [8]. The evidence clearly illustrate the fact *TS* winds are not characterized by a generic vertical velocity profile, but by a family of profiles, depending on the distance from the location of interest to the path of the storm. In addition, since the causative cloud is typically in motion, the issue is further complicated by the fact that at least one additional factor should be considered, which is the ratio between the translational velocity of the cloud and the downdraft wind velocity.

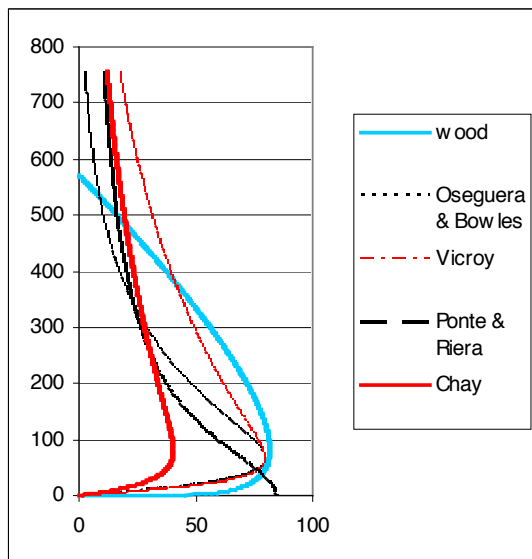


Fig.5. Vertical profile at radius $r = 100\text{m}$

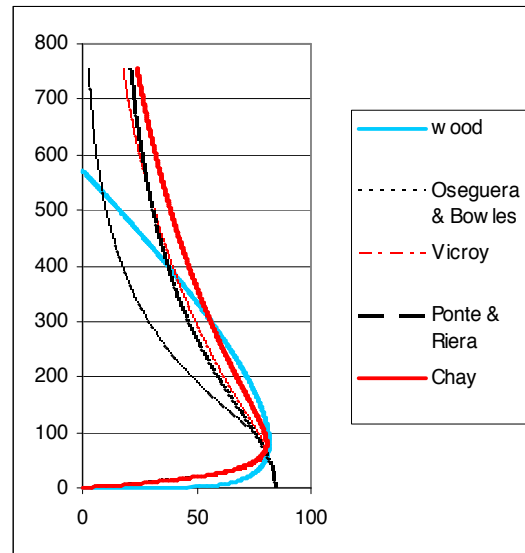


Fig.6- Vertical profile at radius $r = 200$

6. FLUCTUATING VELOCITY COMPONENT

Under usual conditions, atmospheric flow in the lower boundary layer is turbulent. Turbulence manifests itself as fluctuations of the wind velocity around its average value. The magnitude of the velocity vector in the direction of the flow may be written as:

$$V(t) = V_m(t) + \Delta V(t) \quad (25)$$

In which $V(t)$ denotes the instantaneous velocity at time t , $V_m(t)$ the mean velocity and $\Delta V(t)$ the fluctuating longitudinal velocity component. When the flow is stationary, the mean velocity V_m does not depend on time. In such case, eq. (25) can alternatively be written in the form:

$$V(t) = V_o [1 + I \phi(t)] \quad (26)$$

In which V_o is a mean reference velocity, I the intensity of turbulence and $\phi(t)$ a stationary random process with zero mean and unitary standard deviation. The intensity of turbulence is defined as the quotient between the standard deviation of the longitudinal velocity fluctuations and the mean velocity [26]. The random process $\phi(t)$ is defined by its power spectral density function (psdf), for which a number of models have been proposed in the technical literature, such as those due to Davenport, Von Karman, Kaimal and Harris [4-26]. However, all these spectral density functions are only applicable when vertical stability of the atmosphere prevails and the turbulence in the lower boundary layer results mainly from the interaction of the flow with the rough soil surface. Note that a minimum stretch is needed to develop a given profile and turbulence intensity. The length of this so-called *exposure terrain* is of the order of one kilometer or more, condition that is not satisfied by *TS* winds, in which the flow lines remain close and approximately parallel to the ground for a few hundred meters. Thus, there seems to be no reason to expect that the psdf of the velocity fluctuations in *TS* winds will be satisfactorily modelled by the functions normally employed for *EPS* winds.

A purely empirical approach to the problem seems of little use, on account of the large number of factors discussed in connection with the vertical profile, which should also influence the turbulence spectra. However, a preliminary analysis of *TS* wind records revealed peaks in the psdf's of the fluctuations, in the frequency band between 0,05 and 0,55Hz, with no prevailing frequency. A very simple model for the longitudinal turbulence in *TS* events was then parsimoniously adopted: a band-pass white noise, with frequency limits as quoted above. In order to simulate such process in preliminary applications, the velocity fluctuations were expressed as $V_o I \phi(t)$, with:

$$\phi(t) = A_1(t) \sin(\omega_m t) + A_2(t) \cos(\omega_m t) \quad (27)$$

$$A_1(t) = \sin(\omega_L t) \quad (28)$$

$$A_2(t) = \cos(\omega_L t) \quad (29)$$

In which A_1 and A_2 are functions of the lower cut-off frequency ω_L , while ω_m denotes the median frequency between ω_L and the upper cut-off frequency ω_u , that depends on the power spectral density function to be simulated [14]. Introducing eqs.(28) and.(29) into eq.(27) leads to the equivalent generic equation

$$\phi(t) = a \cos[(\omega_m - \omega_L)t + \theta] \quad (30)$$

in which θ is a random phase angle characterized by a uniform probability distribution function within the $[0, 2\pi]$ interval. Figure 7 shows a sample of the velocity-time function for a *TS* event with characteristic duration $T = 60s$, maximum tangential velocity equal to one and

intensity of turbulence $I = 0,50$. The vertical and horizontal axis represent the velocity in (m/s) and the time in (s) respectively.

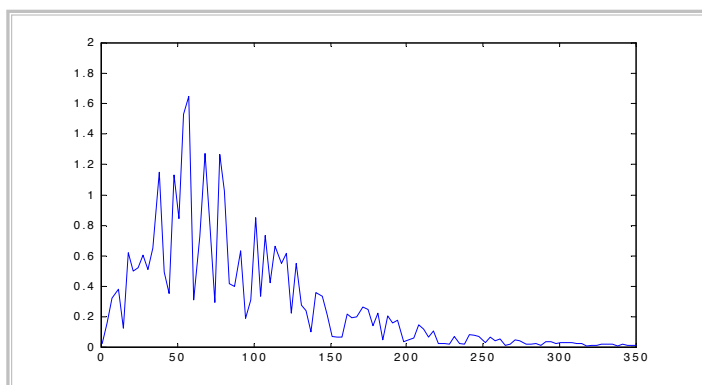


Figure 7. Velocity-time plot for sample *TS* event

5. RANDOM VARIABLES IN SIMULATION OF WIND SERIES

The simulation of annual maximum wind series at predefined locations requires the specification of the following data:

- Geographic region of interest.
- Dimensions of area in which the simulation will be performed
- Mean frequency of *TS* events in the region
- A probabilistic model of the pressure drop
- Probability distribution of intensity and orientation of background wind
- A probabilistic model of the characteristic time of *TS* events
- A probabilistic model of height from ground to cloud .

The topics listed above are discussed in this section in connection with the numerical examples, which aim at demonstrating the feasibility of the approach.

5.1. *Geographic region of interest.* Riera and Nanni [23] present statistical data on extreme wind velocities collected at meteorological stations in South-Eastern Brasil. The recorded velocities were classified as due to *EPS* or *TS* events and processed separately, thus offering reliable direct observational evidence. From those records, Porto Alegre and Uruguiana were selected as test cases to apply the simulation procedure proposed herein.

5.2. *Dimensions of area in which the simulation will be performed* The area considered was a square with sides 20km long. The site where the wind climate will be simulated is located at its centre. The dimensions of the region should be large enough to assure that the probability of a storm path that originates outside the region reaches its centre is negligibly small. Since the shortest distance from the edge of the square to its centre is 10km, this first requirement would be thus satisfied. The second factor is related to the assessment of the frequency of occurrence of *TS* events in the region, which is an importante climatological factor, discussed in Section 5.3, that led to the same length of the sides of the square. In fact, the region considered might also be circular with 10 km radius

5.3. *Mean frequency of TS events in the region.* The simulation procedure requires the specification of the mean number of *TS* events per year in the region under consideration. In the examples this number was determined from data on isoceraunics in brazilian code NBR

5419 (1991). The information is generally available because of its application in electric power transmission. Essentially, it consists of the records of the number of *thunder events*, heard by operators at meteorological stations. Since thunders always occur in connection with fully developed *TS* events, it may be admitted with little error that the *number of isoceraunics equals the number of TS events that may be heard by the operator at the meteorological station*. Thus, admitting that the operator generally misses –that is, does not take notice of– thunder when the causative cloud is farther than about 10km, the choice of the dimensions indicated in Section 5.2, allows adopting the number of isoceraunics as indicative of the mean yeraly number of *TS* events in the region of interest. Table 1 shows the mean number of *TS* events per year in the examples.

Table 1- Isoceraunics in Porto Alegre and Uruguaiana

Station	Mean number of <i>TS</i> events/ year
Porto Alegre	20
Uruguaiana	30

5. 4. *Pressure drop in thunderstorms.* In Porto Alegre records of pressure drops of up to about 7 milibars per hour (700N/m^2) can be found. Caracena [5] suggests that the pressure drop in microbursts varies from 2,4 mb to 5 mb (240 N/m^2 to 500 N/m^2), but no further indication is given concerning its probability density. In the ensuing simulations a *Gumbel* – (Type I Extreme Value Distribution) with shape an scale parameters $\alpha = 50\text{ N/m}^2$ and $\gamma = 100\text{ N/m}^2$, respectively, are adopted. The resulting probability density function is shown in Figure 8.

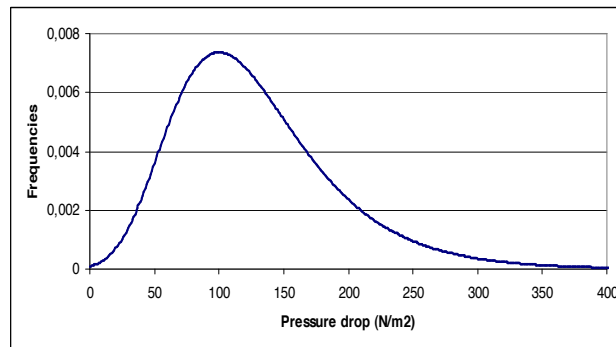


Figure 8 – Probability density function of pressure drop in a random *TS* event

Table 2- Data from brazilian meteorological stations: characteristic time *T*

Station	Date	Characteristic time <i>T</i>	Maximum velocity
Passo Fundo	17/10/90	330 s	15,6 m/s
Passo Fundo	10/02/89	480 s	15,6m/s
Passo Fundo	20/12/87	510 s	18,1m/s
São Luiz Gonzaga	01/07/93	180 s	25m/s
São Luiz Gonzaga	11/11/88	570 s	25,8 m/s
Sao Luiz Gonzaga	05/01/85	210 s	20,8 m/s

5.6. *Characteristic Time.* The characteristic time is the storm duration from its beginning to the moment when the velocity reaches its maximum value. The authors did not find any statistical data on the subject in the literature. Thus, for simulation purposes available TS records from two Brazilian meteorological stations were resorted to. The data is shown in table 2.

The mean value and the standard deviation for the records shown in Table 5.2 are $\mu = 380$ s and $\sigma = 164$ s. The parameters of an extreme type I distribution may be calculated by:

$$\mu = \gamma + 0,577 \alpha \quad (22)$$

$$\sigma = 1,282 \alpha \quad (23)$$

$$\alpha = 127\text{s} \quad (24)$$

$$\gamma = 306 \text{ s} \quad (25)$$

5.5. *A probabilistic model of the background wind velocity.* In the simulation process, the modulus of the background wind velocity at the reference 10m height was assumed to present a Weibull distribution with shape parameter $\beta = 2,5$ and location parameter $\theta = 3,0$ m/s. These values were obtained from 50 years records reported in the Rio Grande do Sul Eolic map. Since no reference was found concerning the background wind orientation, a uniform distribution between 0 to 2π was adopted for the direction of background winds.

5.6. *Height of cumulonimbus cloud.* No statistical data on this parameter was found by the authors. There seems to be no indication of a possible dependence of the parameters on the geographical location. For middle latitudes, as is the case of the stations considered in the examples, a normal distribution with mean $\mu = 10000$ m and standard deviation $\sigma = 500$ m was adopted.

6. SIMULATION METHOD

A procedure to simulate series of maximum annual wind velocities was programmed in MatLab. The simulation adopted the parameters described in section 5 with the results shown in Table 3. The table presents the parameters obtained from series of 50 maximum annual wind velocities. The selected probability distribution, the Kolmogorov and Smirnov (KS) factor for goodness of fit and the mean number of storms per year for each studied location are presented in the table.

Table 3 – Simulation results

Station	TS events per year (n_s)	Mean Value (m/s)	Standard deviation (m/s)	Location parameter γ	Shape parameter	Distribution model	KS Factor DC
Porto Alegre	20	27,00	4,18	25,12	3,26	Type I	0,07
Uruguaiana	30	27,64	3,49	26,08	2,72	Type I	0,05

6.1. *Comparison of simulated records with available observations.* The probability density functions of maximum annual TS winds at the two selected meteorological stations obtained by simulation were compared with predictions based on actual records Riera *et al.* (1989). These references furnish maximum wind velocities for eight orientations (octants). Tables 3

and 4 show the mean, standard deviation and extreme Type I (Gumbel) parameters for TS wind velocities.

Table 4 - Peak Annual TS Wind Velocities (m/s) according to orientation

Octant	Porto Alegre				Uruguaiiana			
	Mean	σ	Gama (γ)	Alfa (α)	Mean	σ	Gama (γ)	Alfa (α)
1	14	3,5	12,42	2,73	13	5	10,75	3,90
2	13	4,0	11,20	3,12	14	4	12,20	3,12
3	16	4,2	14,11	3,28	16	4,8	13,84	3,74
4	20	6	17,30	4,68	21	7	17,85	5,46
5	20	5,8	17,39	4,52	20	6	17,30	4,68
6	21	5,0	18,75	3,90	18	6,5	15,07	5,07
7	19	6,0	16,30	4,68	17	5,8	14,39	4,52
8	17,5	6,3	14,66	4,91	15,5	5	13,25	3,90

Using data from each octant, it is possible to determine the maximum velocities for each station, regardless of wind orientation, indicated in table 5. The density function for the maximum velocities will also be Gumbel with the following parameters:

$$\gamma = \alpha \ln \sum \exp(\gamma_i / \alpha) \quad (26)$$

$$\alpha = \sum \alpha_i / 8 \quad (27)$$

in which γ_i , α_i , denote the parameters for each octant i ($i = 1, \dots, 8$).

Table 5 - Parameters of probability density function of maximum annual TS wind

Station	γ	α
Porto Alegre	24,40	3,97
Uruguaiiana	23,67	4,30

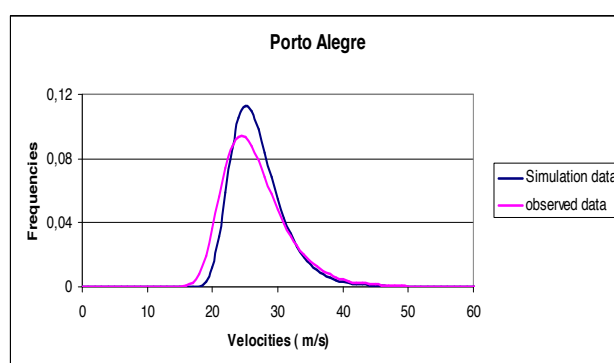


Figure 9 – Probability density functions for maximum annual TS winds in Porto Alegre

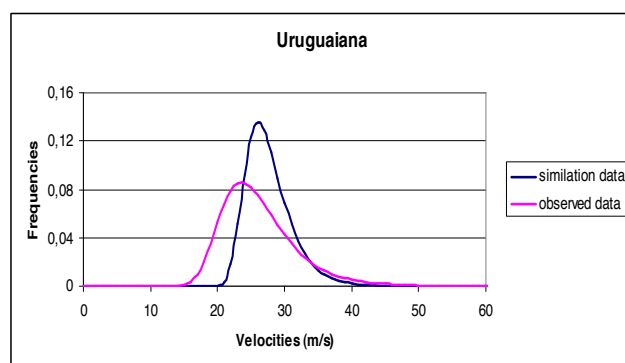


Figure 10 – Probability density functions for maximum annual TS winds (Uruguaiana)

The probability density functions of the maximum annual TS wind velocities at the two meteorological stations considered in this paper, obtained by simulation and direct observation, are shown in Figures 9 and 10. The differences between both sets of results are of the same order as the statistical errors in the latter, which are not negligible due to the short duration of the records (28 years in Porto Alegre and 21 years in Uruguaiana) and may be considered compatible. In summary, a robust model for the wind velocity field during thunderstorms was proposed in the paper, taking into consideration all features of the phenomenon considered relevant for the design of structures subjected to wind action. The model predictions are compatible with available evidence concerning, for example, storm duration or vertical velocity profiles. Moreover, the formulation of the model requires a number of parameters that have ranges of variation reasonably well defined in Meteorology, allowing risk assessments even in situations in which scarce data is available for the region of interest. Presently, studies are being conducted to estimate the risk of intense TS winds in the Amazon region, which are needed for the design of TL crossings in uninhabited areas.

7. ANALYSIS OF DOWNBURST EVENT

The wind fields in extra-tropical cyclons as well as in tropical storms may be modelled, for purposes of structural analysis and design, as stationary random processes, in which the mean wind velocity at the reference 10m height may be assumed constant over a large area. On the other hand, downburst winds and tornadoes are characterized by a pronounced spatial variability as well as by their transient nature. In consequence, records of TS winds are scarce and much needed to contrast with theoretical or numerical models and predictions such as those discussed in the previous sections. One example will be discussed next. The measurements were conducted at the 40m high tower of the Universidade de Passo Fundo (UPF), RS, Brasil, meteorological station. Cup anemometers are installed at levels 10, 20, 30 and 40m above ground. The wind orientation is measured only at elevation 40m. Figure 11 shows a Google plan view of the station and surrounding area, as well as the location of the tower of the UPF TV station, destroyed during a TS event on November 9, 2007. The meteorological station is situated at $28^{\circ} 13' 35''$ S and $52^{\circ} 23' 03''$ W, at an altitude of 692m.

Fig. 13 presents a view of the velocity records at 20, 30 and 40m, respectively, while Fig. 14 presents the wind orientation, recorded at 40m. It may be clearly seen that the storm was nearly stationary - the background wind velocity at 40m height remains well below 5m/s during the minutes preceding the storm – meaning that the causative cloud approaches the



Figure 11. Plan view of meteorological station (center down) as well as UPF TV station

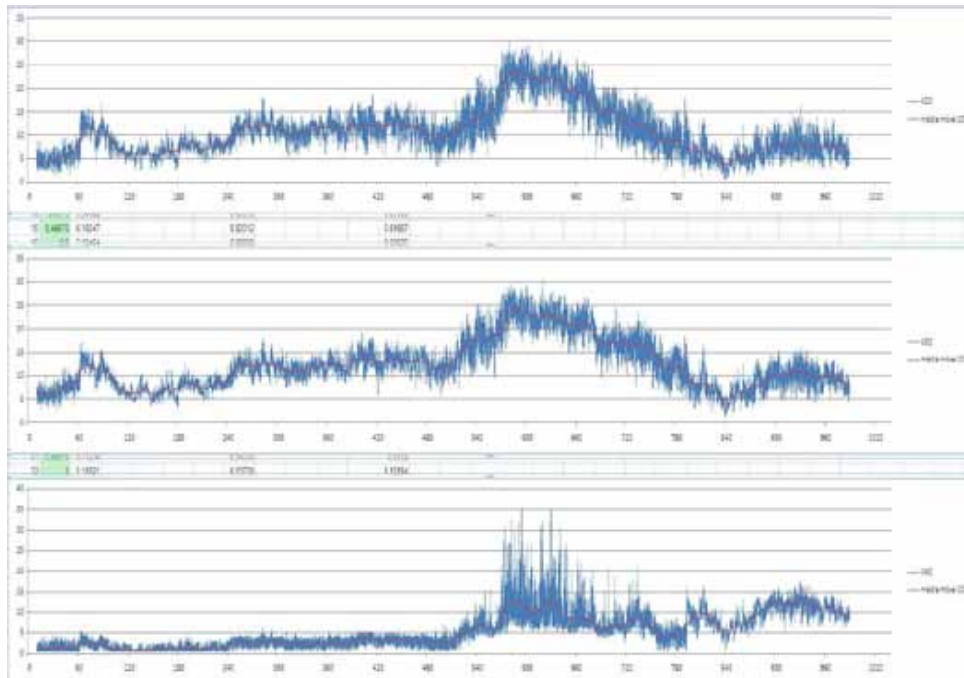


Figure 12. Wind velocity records at 20, 30 and 40m height. The instrument at 10m was out of order

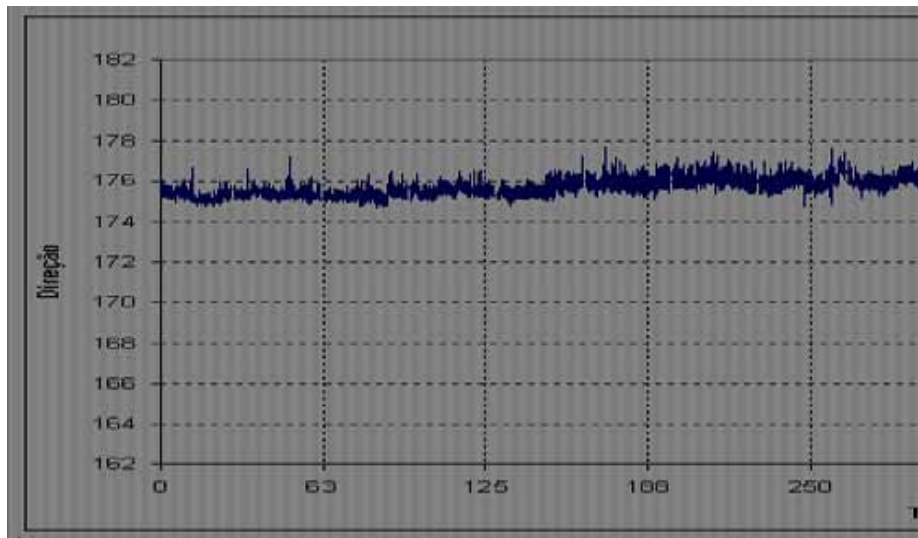


Figure 13. Instantaneous orientation of the wind horizontal component at 40m height

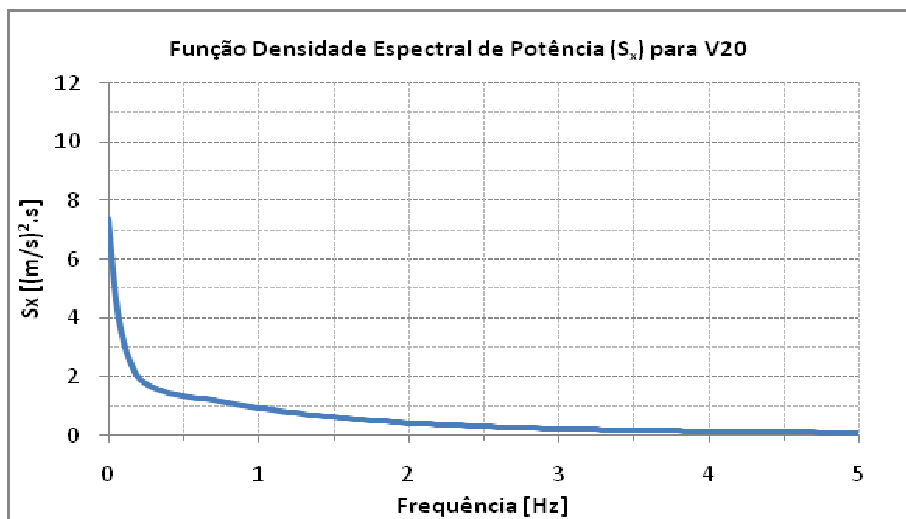


Figure 14. Power spectral density function of fluctuating component at 20m level ($\Delta t = 30s$)

station slowly [3]. Moreover, up to around $t = 500$ s there is no indication of the arrival on the wind front, which affects only layers *below* the 40m level.

Note that the time scale of the velocity records is out of phase with the scale of the orientation record, in which the *TS* wind front may be seen to arrive at $t = 375$ s . It seems also evident that between $t = 575$ s and $t = 735$ s the operation of the anemometer installed at 40m was disturbed by the strong vertical velocity components of the downburst. This will require wind tunnel measurements with the middle plane of the cup anemometer inclined in relation to the wind orientation, to assess the influence of the orientation.

Finally, another issue that requires further assessment is related to the *fluctuating components* of the velocity field. A *mean velocity* record was obtained by means of a

moving average over a period Δt and a fluctuating component defined as the difference between the measured velocities and the mean. A preliminary plot of the power spectral density function of the fluctuating component in the interval between 360 and 985s, assumed to be a sample of a stationary random process, is shown in Figure 15. The rms value of the fluctuating velocity for this record is about 1.7m/s. It is noted that, in agreement with previous evidence registered at the same station, neglecting in this case the record at elevation 40m as an *outlier*, it may be observed that the velocity time-histories at the other two elevations are highly correlated, which also indicates that turbulence *is not* caused by surface roughness.

8. CONCLUSIONS

An overview of ongoing research at LDEC, UFRGS, Brasil, on extreme winds caused by downbursts (*TS* winds) was presented. Initially a semi-empirical model of the wind field in a downburst is described, which aims at the consideration of meteorological variables in the simulation of such events, such as the main features of the cumulonimbus cloud that causes the downdraft. The use of the model to simulate the extreme wind climate at two locations in southern Brasil, where data on annual extreme velocities classified according to the storm type are available, proves that the approach is feasible and might be considered in structural reliability assessments. Finally, to emphasize the need of permanent evaluations of the performance of models to predict wind effects on structures, experimental evidence on the wind field during a *TS* event presently under analysis is finally reported.

ACKNOWLEDGEMENTS

The writer wishes to acknowledge the partial support of CNPq and CAPES (Brazil) and AWES (Australia).

9. References

- [1] ABNT- Associação Brasileira de Normas Técnicas (1987): “*Ação do Vento nas Edificações*”, Norma NBR- 6123, Rio de Janeiro, 1987.
- [2] ABNT- Associação Brasileira de Normas Técnicas (1991) : “*Proteção de estruturas contra descargas atmosféricas*”, NBR – 5419, Rio de Janeiro 1991.
- [3] Bergamini Puglia, V. e Ramires, L.(2010): “Análise de uma tormenta TS”, *Relatório [4] Técnico*, PPGEC, UFRGS, Porto Alegre, RS, Brasil.
- [4] Blessmann, J. (1995), *O Vento na Engenharia Estrutural*, Editora da Universidade, 1ª edição, Porto Alegre, RS, Brasil..
- [5] Caracena,F.,Holle.R.L.and Dosswe IIII, C.A.(1977), *Microbursts: A handbook for visual identification*. NOAA, National Severe Storm Laboratories, U.S.A.,December 1977.
- [6] CIGRÉ SC22 WG16- (2002) Meteorology for overhead lines- *Draft Report on Current Practices regarding Frequencies and Magnitude of High Intensity Winds*- Aug . 2002
- [7] Chay, MT., Albermani, F, Wilson, B.(2006); “Numerical and analytical simulation of downburst wind loads”. *Engineering Structures*, Elsevier, 2006;28:240-254.
- [8] Chen,Ching, L.,Lectchford,C.W.(2004), "A Deterministic-Stochastic Hybrid Model of Downburst and its impact on a Cantilivered Structure", *Engineering Structures*, Elsevier, 2004; 26:619-26.
- [9] Fujita,T.T. (1978), Manual of downburst identification for Project NIMROD, SMPR- 156 . University of Chicago, may 1978.
- [10] Fujita.,T.T (1985), *The Downburst Microburst and Macrobust* – Report of projects NIMROD and JAWS. 1985.

- [11] Gomes, L. and Vickery, B.J. (1976): "On thunderstorm wind gusts in Australia, with particular reference to Observatory Hill, Sydney", *Research Report No. R277*, Civil Engineering laboratory, University of Sydney.
- [12] Holmes, J.D. and Oliver, S.E. (2000): "An empirical model of a downburst", *Engineering Structures*, Elsevier, **22**, 1167-72.
- [13] Holmes, J.D., Baker, C.J., English, E.C., Choi, E.C.C. (2005): "Wind structures and codification", *Wind and Structures*, **8**, N° 4, 235-250.
- [14] Lathi, B.P. (1988): *Sistemas de comunicação*, Editora Guanabara, Rio de Janeiro, Brasil.
- [15] McDonald, Alan T. & Fox, Robert W. (1995). "*Introdução à Mecânica dos Fluidos*", Editora Guanabara Koogan S.A. 4a. Edição. Copyright 1995.
- [16] Oseguera, R.M. and Bowles, R.L. (1988): "A Simple Analytic 3-Dimensional Downburst Model Based on Boundary Layer Stagnation Flow". *NASA Technical Memorandum 100632*, July 1988.
- [18] Paluch, M.J., Toazza, A., Rocha, M.M., Marroquim, A.I. (2003): "O laboratório anemométrico da Universidade de Passo Fundo"; *III Workshop Brasileiro de Micrometeorologia*; UFSM, Universidade Federal de Santa Maria, Santa Maria, RS, Brasil, 201-205, 2003
- [19] Paluch, M.J., Cappellari, T.T.O., Riera, J.D. (2007): "Experimental and numerical assessment of EPS wind action on long span transmission line conductors" *J. of Wind Engineering and Industrial Aerodynamics*, Elsevier, The Netherlands, (to be published).
- [20] Ponte Jr, Jacinto (2006), "Modelagem e Simulação do Campo de Velocidades do Vento em Tormentas Elétricas" *Tese de Doutorado*. Promec, UFRGS., Porto Alegre, RS, Brasil, 2005.
- [21] Ponte Jr, J., Riera, J.D., "Wind Velocity Field during Thunderstorms" (2007). *Wind and Structures*, an International Journal; volume 10; number 3, may 2007
- [22] Riera, J. D., Viollaz, A.J. and Reimundin, J.C. (1977): "Some recent results on probabilistic models of extreme wind speeds", *J. of Industrial Aerodynamics*, Elsevier, The Netherlands, **2**, 271-287.
- [23] Riera, J.D. and Nanni, L.F. (1989): "Pilot study of extreme wind velocities in a mixed climate considering wind orientation", *J. of Wind Engineering and Industrial Aerodynamics*, Elsevier, The Netherlands, Vol. 32, 11-20.
- [24] Riera, J.D., Viegas, F.B. and dos Santos, M.L.W. (1989) "Probabilistic assessment of wind loading for structural analysis", *Proceedings, 5th International Conference on Structural Safety and Reliability, ICOSSAR '89*, Innsbruck, Austria, Vol. 1, 55-62, A.A. Balkema, Rotterdam, 1989.
- [25] Riera, J.D. and Rocha, M.M. (1998): "Load definition for wind design and reliability assessments; extreme wind climate", in *Wind Effects on Buildings and Structures*, (J.D. Riera & A.G. Davenport, Editors), A.A. Balkema, Rotterdam, 1998.
- [26] Simiu, E. and Scanlan, R.H.: *Wind Effects on Buildings and Structures*, Third Edition, John Wiley & Sons, Inc., New York, USA, 1996.
- [27] Thom, H.C.S. (1967): "Toward a universal climatological extreme wind distribution", *Wind Effects on Buildings and Structures*, Ottawa, Canada, Univ. of Toronto Press, Vol. 1, 669-684.
- [28] Vicroy, D.D. (1991) "A Simple, Analytical, Axisymmetric Microburst Model for Downdraft Estimation", *NASA TM-104053*, DOT/FAA/RD, 91/10, Feb-1991.
- [29] Vicroy, D.D. (1992), "Assessment of Microburst Models for Downdraft Estimation", *Journal of Aircraft*, **29**, 1043-8
- [30] Wood, G.S., and Kwok, C.S. (1998), "An empirically derived estimate for the mean velocity profile of a thunderstorm downburst", *7th AWES Workshop*, Auckland, Australia, 1998
- [31] Zhu, S. and Etkin, B. (1985): "Model of the wind field in a downburst", in *Journal of Aircraft*, **22**, N° 7, 595-601, July 1985

Sites references

WW 2010 on line Gides. University of Illinois .

[http://ww2010.atmos.uiuc.edu/\(Gh\)/guides/mtr/svr/comp/out/micro/home.rxml](http://ww2010.atmos.uiuc.edu/(Gh)/guides/mtr/svr/comp/out/micro/home.rxml)